JES
JOURNAL OF ENVIRONMENTAL SCIENCES
ISSN 1001-0742
CN 11-2629/X
June 1, 2013 Volume 25 Number 6
www.jesc.ac.cn

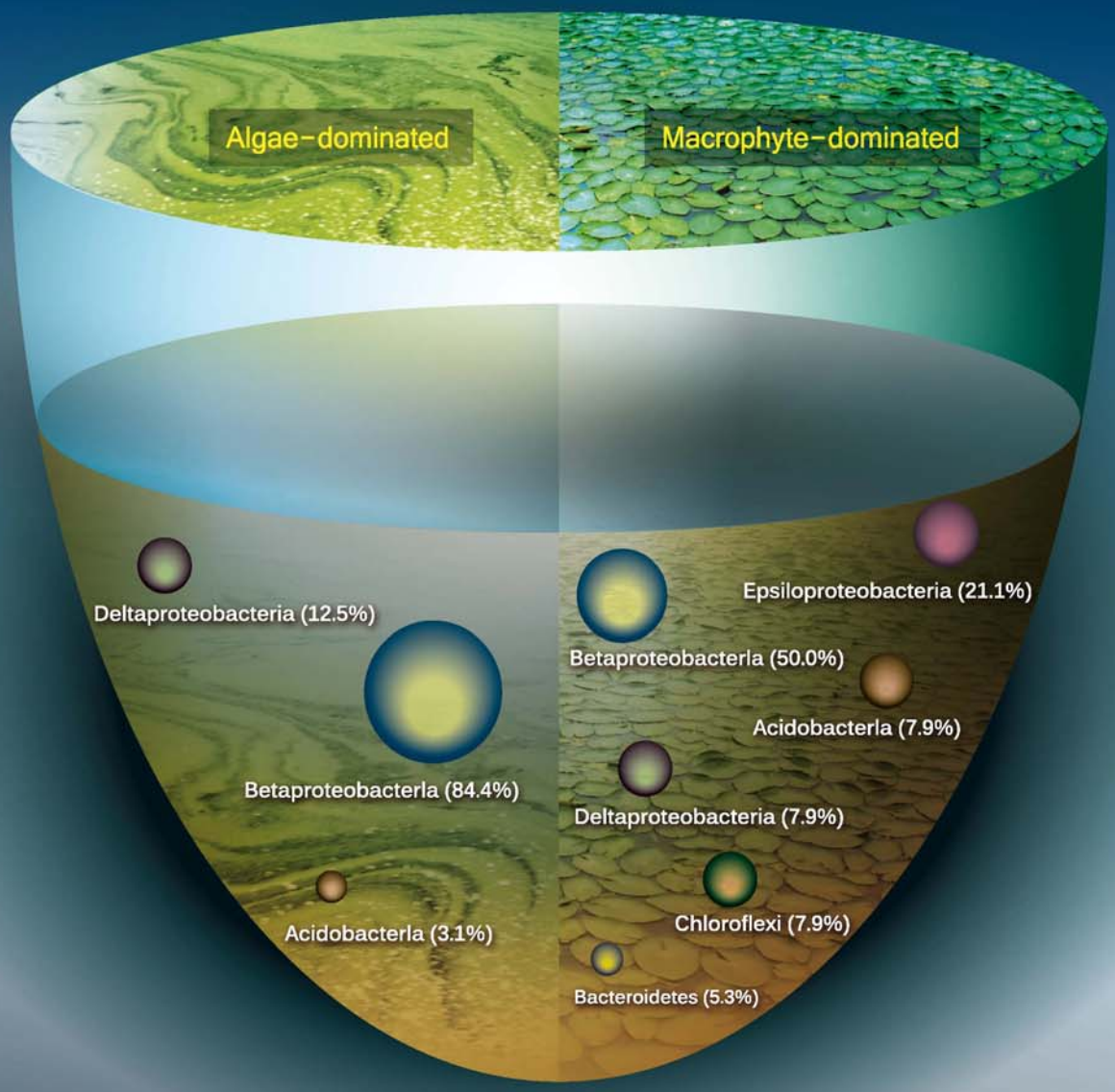

ELSEVIER
Science Press

Sponsored by
Research Center for Eco-Environmental Sciences
Chinese Academy of Sciences

ISSN 1001–0742 **Journal of Environmental Sciences** Vol. 25 No. 6 2013

CONTENTS

Environmental biology

Environmental catalysis and materials

Environmental analytical methods

Serial parameter: CN 11-2629/X*1989*m*207*en*P*25*2013-6

Available online at www.sciencedirect.com
ScienceDirect
Journal of Environmental Sciences 2013, 25(6) 1213–1225
JOURNAL OF ENVIRONMENTAL SCIENCES
ISSN 1001-0742
CN 11-2629/X
www.jesc.ac.cn

Efficient visible light photo-Fenton-like degradation of organic pollutants using *in situ* surface-modified $BiFeO_3$ as a catalyst

Junjian An[1], Lihua Zhu[1], Yingying Zhang[2], Heqing Tang[2,*]

1. College of Chemistry and Chemical Engineering, Huazhong University of Science and Technology, Wuhan 430074, China. E-mail: anjunjian0000@163.com
2. Key Laboratory of Catalysis and Materials Science of the State Ethnic Affairs Commission and Ministry of Education, College of Chemistry and Materials Science, South-Central University for Nationalities, Wuhan 430074, China

Received 11 September 2012; revised 25 December 2012; accepted 28 December 2012

Abstract

The visible light photo-Fenton-like catalytic performance of $BiFeO_3$ nanoparticles was investigated using Methyl Violet (MV), Rhodamine B (RhB) and phenol as probes. Under optimum conditions, the pseudo first-order rate constant (k) was determined to be 2.21×10^{-2}, 5.56×10^{-2} and 2.01×10^{-2} min^{-1} for the degradation of MV (30 μmol/L), RhB (10 μmol/L) and phenol (3 mmol/L), respectively, in the $BiFeO_3$-H_2O_2-visible light (Vis) system. The introduction of visible light irradiation increased the k values of MV, RhB and phenol degradation 3.47, 1.95 and 2.07 times in comparison with those in dark. Generally, the k values in the $BiFeO_3$-H_2O_2-Vis system were accelerated by increasing $BiFeO_3$ load and H_2O_2 concentration, but decreased with increasing initial pollutant concentration. To further enhance the degradation of pollutants at high concentrations, $BiFeO_3$ was modified with the addition of surface modifiers. The addition of ethylenediamineteraacetic acid (EDTA, 0.4 mmol/L) increased the k value of MV degradation (60 μmol/L) from 1.01×10^{-2} min^{-1} in the $BiFeO_3$-H_2O_2-Vis system to 1.30 min^{-1} in the EDTA-$BiFeO_3$-H_2O_2-Vis system by a factor of 128. This suggests that *in situ* surface modification can enable $BiFeO_3$ nano-particles to be a promising visible light photo-Fenton-like catalyst for the degradation of organic pollutants.

Key words: nanoscale $BiFeO_3$; visible light; photo-Fenton-like catalysis; degradation; surface modification
DOI: 10.1016/S1001-0742(12)60172-7

Introduction

Advanced oxidation processes (AOPs) which revolve around the generation of strongly oxidizing hydroxyl free radicals (·OH) are important processes for decomposing organic pollutants Generally, the activation of H_2O_2 is necessary to generate ·OH radicals. Ultraviolet light (Guo et al. 2010; Dwyer et al., 2008) and ultrasonic (Seitelska et al., 2004; Bremner et al., 2009) irradiation are able to activate H_2O_2. A typical Fenton process uses ferrous ions to activate H_2O_2. Classic Fenton processes require operation at low pH values (pH < 3), due to the production of iron sludge at higher pH values. To overcome this drawback, chelating agents such as ethylenediamineteraacetic acid (EDTA), oxalic acid, citric acid and tartaric acid can be added to prevent the formation of iron sludge (Li et al., 2005; Monteagudo et al., 2008; Rastogi et al., 2009; Kwon et al., 2009; Nam et al., 2001; Roy et al., 2003). Such modifications lead to the construction of homogeneous Fenton-like processes, which allow higher operating pH values. Moreover, ultraviolet light irradiation (Han et al., 2008), visible-light irradiation (Cheng et al., 2004; Zepp et al. 1992; Chen et al., 2001; Malato et al., 2007), ultrasonic irradiation, microwave irradiation, and electrolysis (Tokumura et al., 2008; Yang et al. 2009; Ma et al., 2010; Ventura et al., 2002) can be used in homogenous Fenton and Fenton-like processes to enhance the degradation of organic pollutants.

Recently, increasing attention has been paid to heterogeneous Fenton-like catalysts. It was found that the degradation of pollutants in soil could be achieved through the use of H_2O_2, which was activated by the crude iron ore in soil (Yuan et al., 2006). Because of their large specific surface areas, nanoscale iron-containing heterogeneous catalysts have been extensively investigated, including Fe_3O_4 (Zhang et al., 2008), iron-loaded zeolites and exchange resins (Feng et al., 2004; Neamtu et al., 2004; Catrinescu et al., 2003), and metallic element-doped iron oxides (Deng et al., 2008; Guimaraes et al., 2009; Heckert

* Corresponding author. E-mail: hqtang62@yahoo.com.cn

et al., 2008). Besides heterogeneous Fenton-like catalysts, photocatalysts have also attracted much attention, such as TiO_2 with or without surface modification (Yu et al., 2003; Zhang et al., 2010; Cai et al., 2009; He et al., 2009).

Our recent work reported that nanoscale $BiFeO_3$ as a heterogeneous Fenton-like catalyst could activate H_2O_2 to degrade Rhodamine B (RhB) effectively in the dark over a wide pH range (Luo et al., 2010). Nevertheless, we found that the catalytic ability of nanoscale $BiFeO_3$ was not high enough to degrade more stable organic pollutants (e.g., bisphenol A and Methyl Violet (MV)), which motivated us to develop effective means of improving the catalytic ability of $BiFeO_3$ nanoparticles either by introducing *in situ* surface modification or through photoirradiation. We noted that nanoscale $BiFeO_3$ has been explored as a photocatalyst for water splitting and degradation of organic pollutants due to its small band gap (2.10 eV) (Huo et al., 2010; Liu et al., 2010; Li et al., 2009; Gao et al. 2007). It is still a challenge to increase the photocatalytic activity of $BiFeO_3$ for its application in the field of photocatalytic oxidation. Guo and coworkers prepared Gd-doped $BiFeO_3$ nanoparticles with enhanced photocatalytic activity, due to an anomalously high dielectric constant at the rhombohedral-orthorhombic phase boundary that enlarges the space-charge region at the interface of the particle and solution (Guo et al., 2010) Considering that H_2O_2 as an appropriate electron acceptor can significantly increase the degradation and mineralization of organic pollutants over TiO_2 photocatalysts (Wang et al., 2009), it was expected that the simultaneous use of H_2O_2 and $BiFeO_3$ nanoparticles could accelerate the degradation of organic pollutants under visible light irradiation. Moreover, appropriate surface modification able to increase the catalytic ability of $BiFeO_3$ nanoparticles in the dark was also expected to enhance the photocatalytic performance of $BiFeO_3$ nanoparticles. Therefore, the main objective of the present work is focused on the integration of photocatalysis and Fentonlike catalysis through the use of $BiFeO_3$ nanoparticles as a heterogeneous photocatalyst, organic ligands as surface modifiers, and H_2O_2 as both a green electron acceptor and oxidant.

1 Experimental

1.1 Chemicals and materials

Iron nitrate ($Fe(NO_3)_3{\cdot}9H_2O$), bismuth nitrate ($Bi(NO_3)_3{\cdot}5H_2O$) and citric acid were obtained from Tianjin Chemical (Tianjin, China). Ethylene glycol monomethyl ether, nitric acid, methyl violet 6B, RhB, 30% (*W*/*W*) H_2O_2 and nitrilotriacetic acid (NTA) were provided by Sinopharm Chemical Reagent Co., Ltd. (Shanghai, China). Ethylene glycol and phenol were obtained from Shanghai No.4 Reagent & H.V. Chemical Co., Ltd. (Shanghai, China). Coumarin was obtained from Shenyang No.3 Chemical Reagent Factory (Shenyang, China). $Na_2HPO_4{\cdot}12H_2O$, KH_2PO_4 and EDTA were provided by Shanghai Zhanyun Chemical Co., Ltd. (Shanghai, China). All chemicals were analytical grade reagents and used without further purification

1.2 Preparation of $BiFeO_3$ nanoparticles

$BiFeO_3$ nanoparticles were prepared with a sol-gel process as reported previously (Luo et al., 2010). Iron nitrate (0.008 mol) and bismuth nitrate (0.008 mol) were dissolved in 2-methoxyethanol (20 mL), followed by adding 20 μL HNO_3 (0.1 mol/L). After citric acid (0.008 mol) and ethylene glycol (10 mL) were added to the solution, the mixture was stirred for 1 hr at 60°C to form a sol. The sol was heated for 5 hr at 100°C to form a brown viscous resin, which was then heated for 30 min in an electric furnace and calcined at 500°C for 2 hr in a muffle furnace. After being cooled down to room temperature, the product was ground to a powder and stored for use.

For surface characterization, $BiFeO_3$ nanoparticles modified with NTA and EDTA were prepared as follows: $BiFeO_3$ nanoparticles (0.025 g) were added to a solution of NTA (0.6 mmol/L) or EDTA (0.4 mmol/L), followed by stirring for 0.5 hr. The solids in the reaction solution were obtained by filtering and fully washing with distilled water until the UV-Vis spectrum (from 200–800 nm) of the filtrate was the same as that of distilled water. The solids were dried at 60°C in an oven for 2 hr and then at 60°C in a vacuum drying oven for 2 hr. The final products were correspondingly referred to as $BiFeO_3$-NTA and $BiFeO_3$-EDTA nanoparticles.

1.3 Degradation experiment

The degradation experiment was carried out in a cylindrical Pyrex vessel at 25°C. Typically, a given amount of $BiFeO_3$ nanoparticles was dispersed in a solution of organic pollutant (50 mL; 30 or 60 μmol/L MV 10 μmol/L RhB, or 3 mmol/L phenol) by sonicating for 1 min, followed by adjusting the pH to 5.0 for MV and RhB or pH 3.0 for phenol with 0.1 mol/L HCl or NaOH. The dispersion was magnetically stirred for 30 min to achieve adsorption-desorption equilibrium between the catalyst and pollutant. A small volume (1.5 mL) of the dispersion was sampled and immediately centrifuged at 14,000 r/min on an EBA-21 centrifuge (Hettich, Germany) to separate $BiFeO_3$ from the solution. The pollutant concentration in the supernatant was measured and taken as its initial concentration. After H_2O_2 was added to the solution, the photocatalytic degradation was initiated by switching on a 500 W halogen lamp with a cutoff filter ($\lambda > 420$ nm). At given time intervals, aliquots of the solution (1.5 mL) were sampled to centrifuge tubes containing a certain quantity of absolute ethyl alcohol (to quench ·OH radicals). After being centrifuged at 14,000 r/min and the remaining pollutant concentration in the supernatant was determined immediately.

1.4 Characterization and analytical methods

The surface morphology was examined on a FEI Sirion-200 scanning electron microscope (SEM). Powder X-ray diffraction (XRD) analysis was performed on a Bruker D8 Advance diffractometer with Cu K_α radiation equipped with a graphite monochromator. Brunauer-Emmett-Teller (BET) surface area was determined by nitrogen adsorption/desorption at 77 K, using a Micrometers ASAP 2020 apparatus. The attenuated total reflection-Fourier transform infrared spectrophotometer (ATR-FT-IR) spectra of $BiFeO_3$, $BiFeO_3$-NTA and $BiFeO_3$-EDTA nanoparticles were recorded on a VERTEX 70 FT-IR infrared spectrometer. The Zeta potentials of $BiFeO_3$, $BiFeO_3$-NTA and $BiFeO_3$-EDTA in the dispersions ($BiFeO_3$ dose 0.5 g/L, NTA concentration 0.6 mmol/L, or EDTA concentration 0.4 mmol/L) at 25°C were measured using a NanoZS zeta Potential meter.

The dye concentration was determined spectrophotometrically on a Varian Cary 50 UV-Visible spectrophotometer. The concentration of phenol was determined with high-performance liquid chromatography (HPLC) on a HPLC system which consisted of Jasco PU-2089 quaternary gradient pumps with a Jasco UV-2075 Intelligent UV/Vis detector. The system was equipped with an automatic sample injector (Rheodyne, Cotati, CA, USA) with a 20-μL loop. An Amethyst C18P column (5 μm, 4.6 × 250 mm) was employed as separation column. In the HPLC experiments, a mixture of methanol and water (40:60, *V*/*V*) with a flow rate of 1.0 mL/min was used as mobile phase. It was filtered through a 0.2 μm filter prior to use. The UV detector was operated at 275 nm. The generation of ·OH was evaluated using the coumarin probe method (Guan et al., 2008), in which the fluorescent intensity of the product 7-hydroxycoumarin from the oxidation of coumarin (1 mmol/L) by the attack of ·OH radicals was recorded on a Jasco FP-6200 fluorescence spectrophotometer. The UV-Vis diffuse reflectance spectrum (DRS) was recorded on an UV-3100 UV-Vis spectrophotometer (Hitachi) with an integrating sphere attachment Fe and Bi contents were monitored by atomic absorption spectroscopy (AAS, Analyst 300, P.E. Inc.). H_2O_2 was measured using the DPD method reported by Bader et al. (1988). The EDTA concentration was measured by ion chromatography (ICS-1500 Dionex, IC). An AS-23 column was employed as separation column. In the IC experiment, KOH solution (28.0 mmol/L) with a flow rate of 1.0 mL/min was used as mobile phase.

2 Results and discussion

2.1 Characterization of $BiFeO_3$, $BiFeO_3$-NTA and $BiFeO_3$-EDTA nanoparticles

The SEM image of $BiFeO_3$ is shown as **Fig. 1a**. It was found that $BiFeO_3$ exhibited a structure composed of nanoparticles with grain sizes of 100–150 nm. The XRD pattern of $BiFeO_3$ (**Fig. 1b**) showed a highly crystalline and single-phase perovskite structure (JCPDS File No. 20–169) and all the peak-splitting suggests that it was rhombohedral. **Figure 1c** shows the nitrogen sorption isotherms at 77K for $BiFeO_3$ nanoparticles. The adsorption at higher P/P_0 was characteristic of a Type H3 loop, indicative of its meso- and macro-porous characteristics. The BET analysis revealed that the specific surface area of $BiFeO_3$ was 7.50 m^2/g, being close to that previously reported (Luo et al., 2010).

The UV-Vis diffuse reflectance spectra of $BiFeO_3$, $BiFeO_3$-NTA and $BiFeO_3$-EDTA nanoparticles are shown in **Fig. 2A**. The $BiFeO_3$ nanoparticles were found to absorb light over the whole tested region ranging from 200 to 800 nm (**Fig. 2A**). This is consistent with the previous observation that $BiFeO_3$ nanoparticles showed photocatalytic performance under both UV and visible light irradiation (Huo et al., 2010; Liu et al., 2010; Li et al., 2009; Gao et al., 2007), although the reported photocatalytic activity was rather low. The $BiFeO_3$ samples modified by NTA and EDTA absorbed light more strongly than that without modification over the whole tested region ranging from 200 to 800 nm. The corresponding values of the direct band gap of $BiFeO_3$, $BiFeO_3$-NTA and $BiFeO_3$-EDTA nanoparticles were evaluated by extrapolating the linear portion of $(\alpha hv)^2$ vs. (hv). The band gap energy of $BiFeO_3$ was about 2.05 eV, which was in good agreement with that reported previously (Huo et al., 2010). The values of the band gap energy of $BiFeO_3$-NTA and $BiFeO_3$-EDTA were

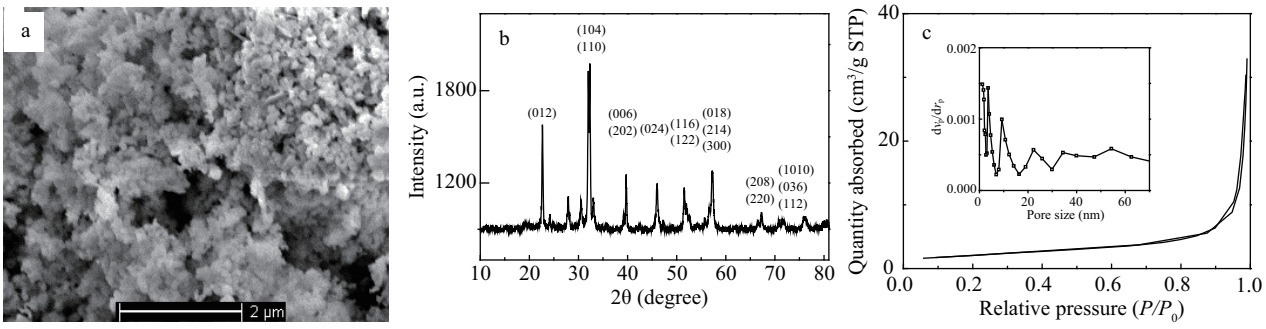

Fig. 1 SEM image (a) and XRD patterns (b) of $BiFeO_3$ nanoparticles, and nitrogen sorption isotherms for $BiFeO_3$ nanoparticles (c). The inset shows the corresponding pore-size distribution.

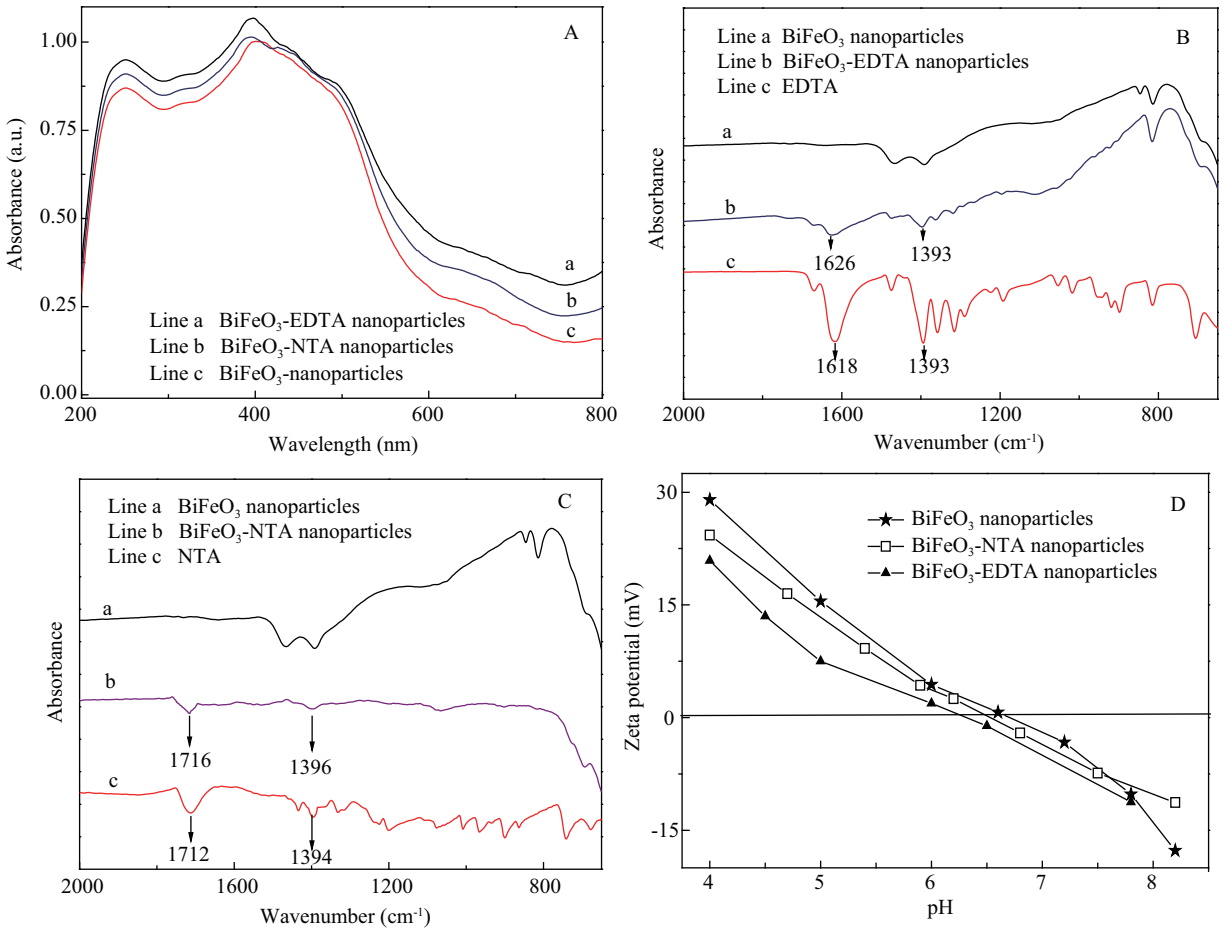

Fig. 2 (A) UV-Vis diffuse reflectance spectra of $BiFeO_3$, $BiFeO_3$-NTA and $BiFeO_3$-EDTA nanoparticles, (B) ATR-FT-IR spectra of $BiFeO_3$, $BiFeO_3$-EDTA and EDTA, (C) ATR-FT-IR spectra of $BiFeO_3$, $BiFeO_3$-NTA and NTA, (D) Zeta potentials of $BiFeO_3$, $BiFeO_3$-NTA and $BiFeO_3$-EDTA at different pH values.

about 1.85 and 1.80 eV, respectively, lower than that of $BiFeO_3$. This hints that surface modification can improve the UV and visible light absorption ability of $BiFeO_3$.

In order to confirm the surface complexing effects of NTA and EDTA, the ATR-FT-IR spectra of $BiFeO_3$, EDTA, $BiFeO_3$-EDTA, NTA and $BiFeO_3$-NTA were measured as shown in **Fig. 2B** and **C**. For EDTA, the absorption peaks at 1618 and 1393 cm^{-1} represent the asymmetrical and symmetrical stretching vibrations of C=O ($\nu_{C\text{-}O}{}^{as}$ and $\nu_{C\text{-}O}{}^{s}$); the band at 1357 cm^{-1} is attributed to the in-plane bending vibration of -NH- ($\delta_{N\text{-}H}$); the bands at 1312 and 1289 cm^{-1} represent the bending vibration of C–H ($\delta_{C\text{-}H}$) and stretching vibration of C–N ($\nu_{C\text{-}N}$), respectively. For NTA, the absorption peaks at 1712 and 1394 cm^{-1} represent $\nu_{C\text{-}O}{}^{as}$ and $\nu_{C\text{-}O}{}^{s}$ of C=O, respectively. In comparison with that without surface modification (**Fig. 2B**), the spectrum of $BiFeO_3$ modified with EDTA gives remarkably strong peaks at 1626 and 1393 cm^{-1}, which in turn correspond to $\nu_{C\text{-}O}{}^{as}$ and $\nu_{C\text{-}O}{}^{s}$ of C=O. The spectrum of $BiFeO_3$ modified with NTA gives weaker absorption peaks at 1716 and 1396 cm^{-1}, which correspond to the peaks for $\nu_{C\text{-}O}{}^{as}$ and $\nu_{C\text{-}O}{}^{s}$ of C=O in the NTA molecule (**Fig. 2C**). The ATR-FT-IR analysis confirmed that NTA and EDTA modified the surface of $BiFeO_3$ successfully. There is a blue shift of 8 or 4 cm^{-1} for the asymmetrical stretching vibration ($\nu_{C\text{-}O}{}^{as}$) of C=O, which may be attributed to direct complexation of the carboxyl in NTA and EDTA with Fe at the $BiFeO_3$ surface to form C–O–Fe bonds, resulting in the enhancement of the bond force constants of C–O. This is in accordance with the conclusion of Guan et al. (2007) concerning the surface complexion of organic carboxylic acids with $Al(OH)_3$. Several works on the surface complexion of carboxylic compounds and ferrites have reported that the difference ($\Delta\nu = \nu_{C\text{-}O}{}^{as} - \nu_{C\text{-}O}{}^{s}$) between the $\nu_{C\text{-}O}{}^{as}$ and $\nu_{C\text{-}O}{}^{s}$ was very important to understand the formation and structure of surface modification. Generally, when $\Delta\nu$ is above 200 cm^{-1}, the carboxyl group coordinates with ferrites in a monodentate form. When $\Delta\nu$ is between 80–150 cm^{-1}, the carboxyl group coordinates with ferrites in a bidentate form (Gao et al., 2009). The $\Delta\nu$ values of $BiFeO_3$-EDTA and $BiFeO_3$-NTA were evaluated to be 233 and 320 cm^{-1}, respectively, indicating that EDTA and NTA were complexing with the $BiFeO_3$ surface in monodentate forms. The C–O–Fe bond was formed in the course of complexation, which shifted the peak of the C=O stretching vibration to higher wavenumbers.

The surface modification of $BiFeO_3$ with NTA and EDTA was further confirmed by comparing Zeta potentials of the three nanoparticulate materials. The catalytic performance of heterogeneous catalysts is not only related to their specific surface area, but also to their surface charge states. Due to the change of Zeta potential after catalysts were modified, the pH of the isoelectric point was altered (Tryba et al., 2009). Therefore, the changes in Zeta potentials before and after the modification can be used to judge the success of the modification. The Zeta potentials of $BiFeO_3$-EDTA, $BiFeO_3$-NTA and $BiFeO_3$ at different pH values were measured as shown in **Fig. 2D**. The pH of the isoelectric point for the three catalysts was determined to be approximately 6.25, 6.48 and 6.7, respectively. In comparison with that of $BiFeO_3$, the pH of the isoelectric point for $BiFeO_3$-NTA and $BiFeO_3$-EDTA were both decreased to some extent. Furthermore, the isoelectric point of $BiFeO_3$-EDTA was shifted to a pH lower than that of $BiFeO_3$-NTA. These may be related to the preparation procedures of the modified catalysts. As the pH value was 5.0, EDTA and NTA in solution both mainly existed in anionic forms. These anions were fixed on the surface of $BiFeO_3$ through surface complexation, which increased the surface negative charges of $BiFeO_3$-NTA and $BiFeO_3$-EDTA. This shifted the isoelectric point of modified $BiFeO_3$ to lower pH. At the same time, because of the stronger complexing ability of EDTA with iron, the amount of anions fixed on the $BiFeO_3$-EDTA surface were more than that on $BiFeO_3$-NTA. Therefore $BiFeO_3$-EDTA carried more negative charges, resulting in the lower pH value for the isoelectric point. The above-mentioned results confirmed that surface complexation occurred on the surface of $BiFeO_3$.

2.2 Visible light photo-Fenton catalytic performance of $BiFeO_3$ nanoparticles

Figure 3 gives the degradation kinetics of MV and RhB in the presence of H_2O_2 and $BiFeO_3$ nanoparticles in the dark and under visible light irradiation. In the dark, the removal of MV within 120 min was 49.8% (**Fig. 3a**), and the removal of RhB within 40 min was 70% (**Fig. 3b**), in comparison with negligible degradation in the absence of $BiFeO_3$ nanoparticles. Therefore, $BiFeO_3$ nanoparticles promote the activation of H_2O_2 in the dark, consistent with our previous report (Luo et al., 2010). However, the much lower removal of MV compared to that of RhB

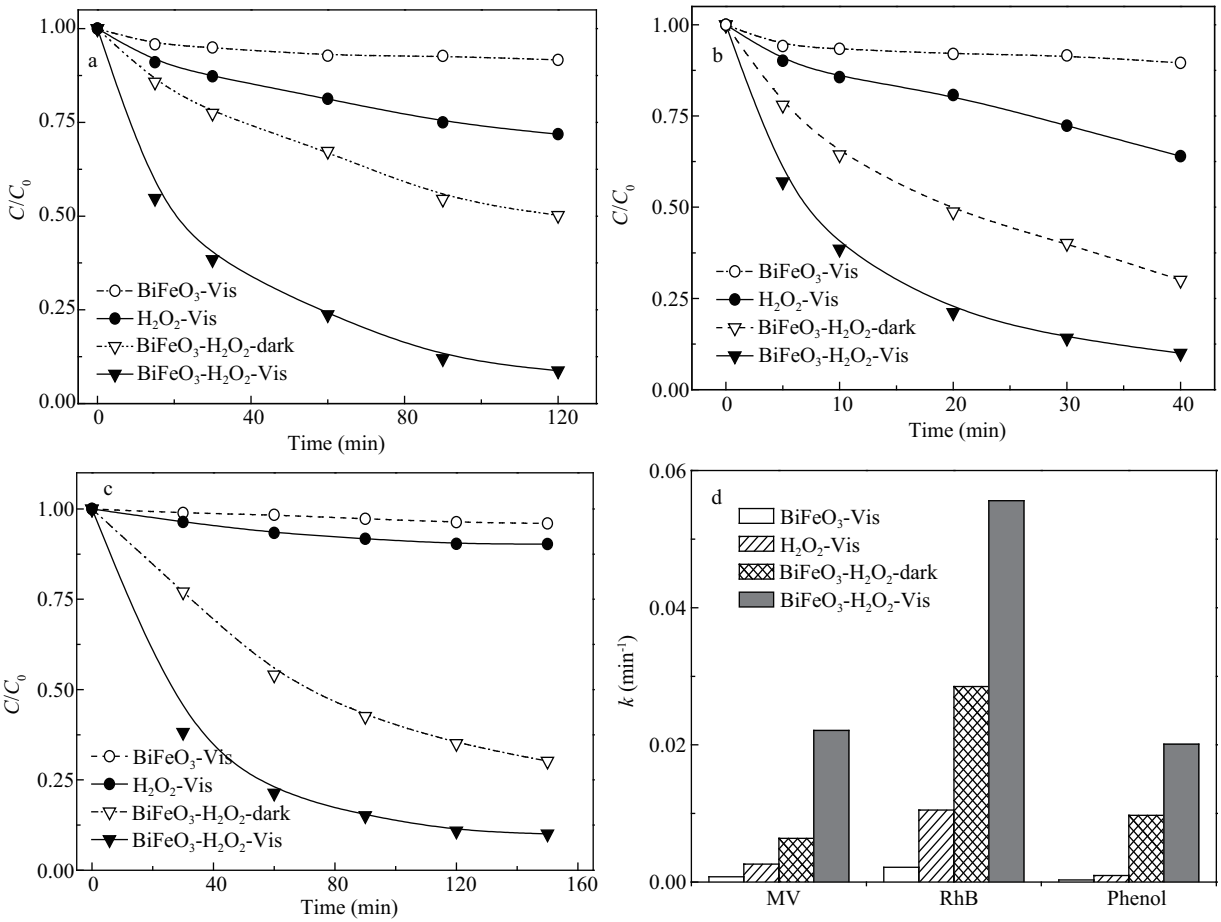

Fig. 3 Degradation of MV (30 μmol/L) (a), RhB (10 μmol/L) (b), phenol (3 mmol/L) (c) and their degradation rate constants in different systems (d). Reaction conditions: $BiFeO_3$ load 0.5 g/L, initial pH 5.0 (MV and RhB) or 3.0 (phenol), temperature 25°C, initial H_2O_2 concentration 20, 10 and 60 mmol/L for the degradation of MV, RhB, and phenol, respectively.

suggests that the catalytic ability of $BiFeO_3$ nanoparticles is not strong enough to degrade more stable pollutants in the presence of H_2O_2 in the dark. By introducing visible light irradiation, the degradation of both RhB and MV was significantly accelerated. For example, the MV removal within 120 min was increased from 49.8% in the dark to 91.3% under visible light irradiation. In control experiments, only 8.4% and 28.1% of the added MV was degraded within 120 min in the $BiFeO_3$Vis and H_2O_2Vis systems, respectively (**Fig. 3a**). These clearly suggest that visible light irradiation can enhance the catalytic ability of $BiFeO_3$ nanoparticles to degrade dyes in the presence of H_2O_2. In other words, $BiFeO_3$ possessed relatively weak visible light photocatalytic ability.

The above-mentioned visible light induced photocatalytic effect may derive from the photosensitization effect of the dye compounds used. To clarify the possible photosensitization effect being induced by the dye compounds, we used colorless phenol as the pollutant instead of dyes. **Figure 3c** shows the degradation kinetics of phenol in different systems. Like the dye compounds, phenol was able to be degraded using H_2O_2 in the presence of $BiFeO_3$ nanoparticles as the catalyst in the dark (**Fig. 3c**) and its degradation was also significantly promoted by introducing visible light irradiation (**Fig. 3c**), which precludes any contribution from the self-sensitized degradation of dyes under visible irradiation. Therefore, it can be concluded that $BiFeO_3$ nanoparticles have strong intrinsic photocatalytic ability for the removal of organic pollutants in the presence of H_2O_2 under visible light irradiation.

The degradation of the tested organic pollutants approximately followed pseudo first-order kinetics, and the values of the degradation rate constants (k) are compared in **Fig. 3d**. It can easily be seen that the k values for each of the tested organic pollutants followed the same order $BiFeO_3$-Vis < H_2O_2-Vis < $BiFeO_3$-H_2O_2-dark < $BiFeO_3$-H_2O_2-Vis. Either $BiFeO_3$ or H_2O_2 alone provided very weak oxidizing ability under visible light irradiation, but $BiFeO_3$ behaved as a good photocatalyst for the activation of H_2O_2 in the decomposition of organic pollutants. In comparison with that in the $BiFeO_3$-H_2O_2-dark system, the k value in the $BiFeO_3$-H_2O_2-Vis system was increased 1.95, 2.07 and 3.47 times for RhB, phenol and MV, respectively. This confirms that the introduction of visible light can provide an alternative approach to enhance the catalytic ability of $BiFeO_3$ nanoparticles for the degradation of refractory organic pollutants in the presence of H_2O_2.

We previously demonstrated that the Fentonlike catalytic ability of $BiFeO_3$ nanoparticles for the degradation of RhB in the presence of H_2O_2 in the dark originated from its enhancing effect on the generation of hydroxyl radicals (Luo et al., 2010). Therefore, a coumarin fluorescent probe (Guan et al., 2008) was employed to evaluate the generation and accumulation of hydroxyl radicals in different systems, where non-fluorescent coumarin was oxidized by hydroxyl radicals to produce fluorescent 7-hydroxycoumarin. As shown in **Fig. 4**, $BiFeO_3$ activated H_2O_2 in the dark to produce hydroxyl radicals. Such activating ability was very much strengthened under visible light irradiation, leading to the generation of a great deal more hydroxyl radicals. This can be explained by the following two factors. On one hand, visible light irradiation accelerates Fenton-like reactions to produce hydroxyl radicals (Cheng et al., 2004; Zepp et al., 1992; Chen et al., 2001; Malato et al., 2007). On the other hand, the adsorbed H_2O_2 scavenges the photo-induced electrons in $BiFeO_3$ to generate hydroxyl radicals (Reaction (1)) (Wang et al., 2009). As a result, in the presence of visible light irradiation and H_2O_2, $BiFeO_3$ nanoparticles catalyze the degradation of organic pollutants remarkably (Reaction (3)) by producing hydroxyl radicals from the photocatalytic (Reaction (1)) and Fenton-like (Reaction (2)) reaction.

$$e^- + H_2O_2 = \cdot OH + OH^- \quad (1)$$

$$\equiv Fe^{II} + H_2O_2 \longrightarrow \equiv Fe^{III} + \cdot OH + OH^- \quad (2)$$

$$Dye + \cdot OH \longrightarrow CO_2 + H_2O + \cdots \quad (3)$$

2.3 Effects of reaction conditions on photocatalytic performance of nano-$BiFeO_3$

The photo-Fentonlike catalytic degradation of organic pollutants over $BiFeO_3$ nanoparticles in the presence of H_2O_2 was influenced by reaction parameters such as catalyst load, H_2O_2 concentration and solution pH, as shown in **Fig. S1**.

As for the effect of catalyst load on the MV degradation, increasing catalyst load initially led to an increased number of reactive sites on the catalyst surface, enhancing generation of ·OH radicals and leading to faster degradation of

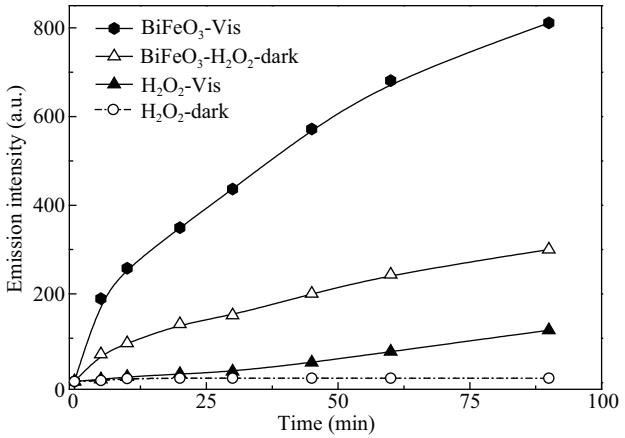

Fig. 4 Reaction time dependence of the fluorescence intensity generated form the oxidation of coumarin by OH radicals in different systems. Reaction conditions: $BiFeO_3$ load 0.5 g/L, solution pH 5, coumarin concentration 1 mmol/L, and initial H_2O_2 concentration 20 mmol/L.

MV. However, superabundant catalyst may produce an excess of ·OH radicals, increasing the reaction between ·OH radicals themselves and then leading to lower efficiency of ·OH radicals for the degradation of organic pollutants. In the case of the photocatalytic catalysis, an excessive catalyst load increases the light filtering effect, which is unfavorable to the catalytic generation of ·OH radicals. Therefore, the optimal load of $BiFeO_3$ nanoparticles was found to be 0.5 g/L.

Similarly, with increasing H_2O_2 concentration, the generation of ·OH radicals was increased, resulting in an increasing k_{MV} value (**Fig. S1b**). However, the decomposition of H_2O_2 at concentrations beyond 20 mmol/L generates an excessive amount of ·OH radicals, which may interact with each other to quench ·OH radicals. In addition a high concentration of H_2O_2 can also scavenge ·OH radicals. All these may result in a decrease in the k_{MV} value. Accordingly, the k_{MV} value was found to reach a maximum at the H_2O_2 concentration of 20 mmol/L.

The effects of pH on the degradation of MV in $BiFeO_3$·H_2O_2 systems were also investigated with and without visible light irradiation (**Fig. S1c**). Over all the tested pH range from pH 3.0 to 9.0, the visible light irradiation significantly enhanced the degradation of MV. As solution pH was increased from 3 to 9, the k_{MV} value was first increased to a maximum at pH 6.0–7.0, and then decreased in the tested $BiFeO_3$-H_2O_2 systems both with and without visible light irradiation. This is different from the pH dependence of RhB degradation in the previously reported $BiFeO_3$-H_2O_2 system (Luo et al., 2010) and the presently investigated $BiFeO_3$-H_2O_2-Vis system, where the k_{RhB} value decreased with increasing pH and the optimal pH value was pH 3.0. Since the inherent H_2O_2-activation ability of $BiFeO_3$ was decreased as solution pH increased from 3 to 9 (Luo et al., 2010), being independent of the dyes used, the above-mentioned different pH dependencies may be attributed to the different adsorption behaviors of the dyes. Indeed, similar pH dependences were observed for the adsorption and degradation of dyes (**Fig. S2a** and **b**). The solution pH affects the surface charge states of $BiFeO_3$ nanoparticles as well as the ionization state of an ionizable dye, and then influences the adsorption of the dye. Because the pK_a of MV was 8.0, MV is predominantly present in the form of a neutral molecule at pH > 8, and is dissociated to positive ions predominantly at pH < 8. At pH values lower than 6.7 (i.e., the isoelectric point of $BiFeO_3$ nanoparticles), the surface of the $BiFeO_3$ nanoparticles becomes positively charged, which is unfavorable to the adsorption of cationic MV due to electrostatic repulsion, thus, the adsorption of MV on the catalyst becomes stronger with increasing pH from 3 to 7. At pH 6.7, the surface of the $BiFeO_3$ nanoparticles is chargeless, and a part of the MV molecule exists in the neutral form, so that the interactions between $BiFeO_3$ nanoparticles and the lone pair electrons of the nitrogen are optimal, thus the adsorbed quantity of MV reached a maximum value of 0.337 mg/g at ca. pH 7. This is similar to the observation of Canle et al., (2005) that the adsorption of aniline and *N*,*N*-dimethyl-aniline on TiO_2 occurred at around 5 to 7 where TiO_2 and the substrates both approximately existed as neutral species. At pH > 6.7, the surface of the $BiFeO_3$ nanoparticles is slightly negatively charged, and the coordinative interaction with amino groups are reduced, resulting in a rapid decrease of the MV adsorption. The adsorption of pollutants on the catalyst not only impacted its Fentonlike performance but also influenced its photocatalytic performance (Fu et al., 2005). Stronger adsorption promotes the degradation rate of pollutants during photocatalysis. Therefore, the photocatalytic performance was also improved by better adsorption of MV on $BiFeO_3$. In contrast, RhB is an acidic dye, which is dissociated to negative ions. Similar reasons will account for the observation that the maximum value of the degradation rate constant for RhB occurs at about pH 3.0.

2.4 Enhancement of photocatalytic ability of nano-$BiFeO_3$ by adding NTA and EDTA

As discussed above, the introduction of visible light irradiation increased the catalytic activity of $BiFeO_3$ nanoparticles for the degradation of both colored and colorless organic pollutants. However, because of the light filtration caused by dyes, it was found that the degradation of dyes became more and more difficult with increasing dye concentration. Therefore, we were interested in further promoting the visible light photo-Fentonlike catalytic ability of $BiFeO_3$ nanoparticles to degrade more resistant pollutants at higher concentrations. As we know, small molecule ligands can strengthen the ability of iron-bearing compounds to activate H_2O_2 or O_2 (Xue et al., 2009; Wang et al., 2010) and the visible light photocatalytic ability of nanoscale TiO_2. Thus, we explored the enhancing effects of NTA and EDTA on the visible light photo-Fentonlike catalytic ability of $BiFeO_3$ nanoparticles.

Figure 5 illustrates the effects of NTA and EDTA on the photo-Fentonlike performance of $BiFeO_3$ nanoparticles for the degradation of MV at a concentration as high as 60 μmol/L. In the $BiFeO_3$-Vis system, only about 6% of MV was removed in 90 min. The addition of either EDTA or NTA to the $BiFeO_3$-H_2O_2 system in the dark greatly enhanced the degradation of MV (**Fig. 5a** and **b**) and the introduction of visible light illumination further significantly accelerated the degradation of MV in the above ligand-containing $BiFeO_3$-H_2O_2 system (**Fig. 5a** and **b**). For example, the removal of MV within 30 sec was dramatically increased from 25% in the EDTA-$BiFeO_3$-H_2O_2-dark system to about 90% in the EDTA-$BiFeO_3$-H_2O_2-Vis system. It was also confirmed that the addition of either EDTA or NTA could not catalyze the H_2O_2 degradation of MV in a visible light-illuminated solution in the absence

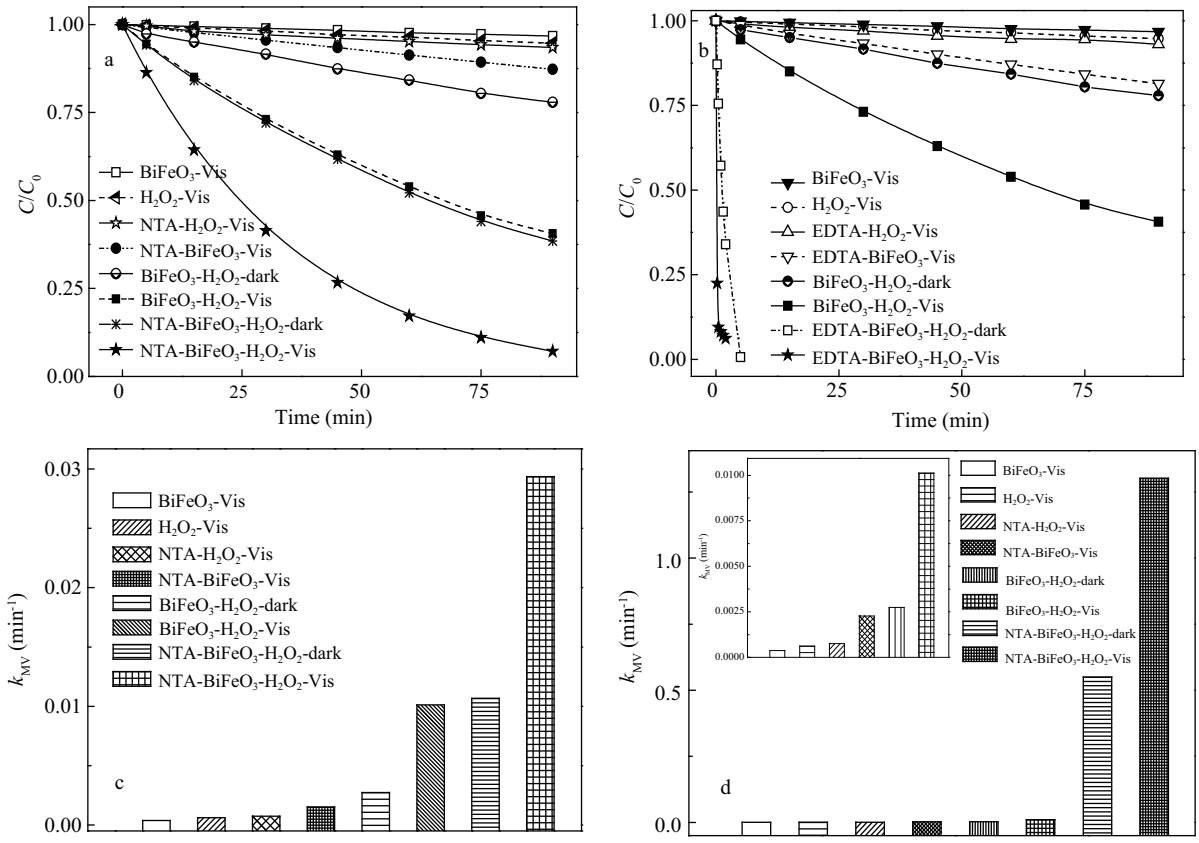

Fig. 5 Effects of ligands of NTA (0.6 mmol/L) (a, c) and EDTA (0.4 mmol/L) (b, d) on degradation kinetics of MV (60 μmol/L) (a, b) and rate constant k_{MV} (c, d). The inset in (d) is the magnification for the related systems. Other reaction conditions: $BiFeO_3$ load 0.5 g/L, H_2O_2 concentration 20 mmol/L, pH 5, and temperature 25°C.

of $BiFeO_3$ nanoparticles (**Figs. 5a** and **b**). Moreover, although ligands can strengthen considerably the photocatalytic performance of $BiFeO_3$ nanoparticles without H_2O_2 (**Figs. 5a** and **b**), the degradation of MV in the ligand-$BiFeO_3$-Vis system was negligible relative to that in the ligand-$BiFeO_3$-H_2O_2-Vis system. The MV degradation in the presence of ligands also followed pseudo first-order reaction kinetics. The fitting of the data in **Fig. 5c** and **d** shows that the apparent rate constant k_{MV} in the different systems is increased in the order $BiFeO_3$-Vis < H_2O_2-Vis, ligand-H_2O_2Vis < ligand-$BiFeO_3$-Vis < ligand-$BiFeO_3$-H_2O_2 < ligand-$BiFeO_3$-H_2O_2-Vis. By comparing with the systems $BiFeO_3$-H_2O_2, $BiFeO_3$-H_2O_2-Vis and ligand-$BiFeO_3$-H_2O_2, it was found that the k_{MV} value in the ligand-$BiFeO_3$-H_2O_2-Vis systems was increased by 9.71, 1.90 and 1.75 times by the addition of NTA, and 473, 128 and 1.36 times by the use of EDTA, respectively. This indicates that the combination of EDTA or NTA with visible light exhibits a strongly synergistic effect on the degradation of MV in the $BiFeO_3$-H_2O_2 system. Furthermore, such a beneficial effect of ligands on the photocatalytic oxidizing ability of the $BiFeO_3$-H_2O_2 system apparently became much more significant at higher concentrations of MV, as will be confirmed by the following discussion.

Figure 6a shows the k_{MV} values of MV degradation at different initial concentrations in the $BiFeO_3$-H_2O_2 system in the absence and presence of EDTA and/or visible light illumination. As the initial MV concentration was increased, the k_{MV} values in all the studied systems decreased. For all concentrations of MV, the introduction of EDTA improved the catalytic activity of $BiFeO_3$ remarkably. To investigate the influence of MV concentration on the synergistic effects of ligands and visible light, the ratio of k_{MV} in the EDTA-$BiFeO_3$-H_2O_2 systems under visible light illumination(k_{MV}^{photo}) to that in the dark (k_{MV}^{dark}) was calculated and is shown in **Fig. 6b**. It can be easily seen that as the initial MV concentration increased from 30 to 240 μmol/L, the value of $k_{MV}^{photo}/k_{MV}^{dark}$ increased from 1.98 to 4.30. This demonstrates that the effect of EDTA on the photocatalytic activity of $BiFeO_3$ nanoparticles becomes much stronger as the initial concentration of MV is increased. In other words, the simultaneous use of EDTA and visible light irradiation can significantly accelerate the degradation of MV in the $BiFeO_3$-H_2O_2 system especially at high concentrations of substrate.

The enhancement effect of ligands on the photo-Fentonlike catalytic performance of $BiFeO_3$ nanoparticles was observed to be dependent on the initial concentration of the ligand itself. With increasing ligand concentration from 0 to 1.0 mmol/L, the values of k_{MV} evaluated at the initial stage of degradation (the first 30 sec) were gradually increased first to a maximum, then decreased

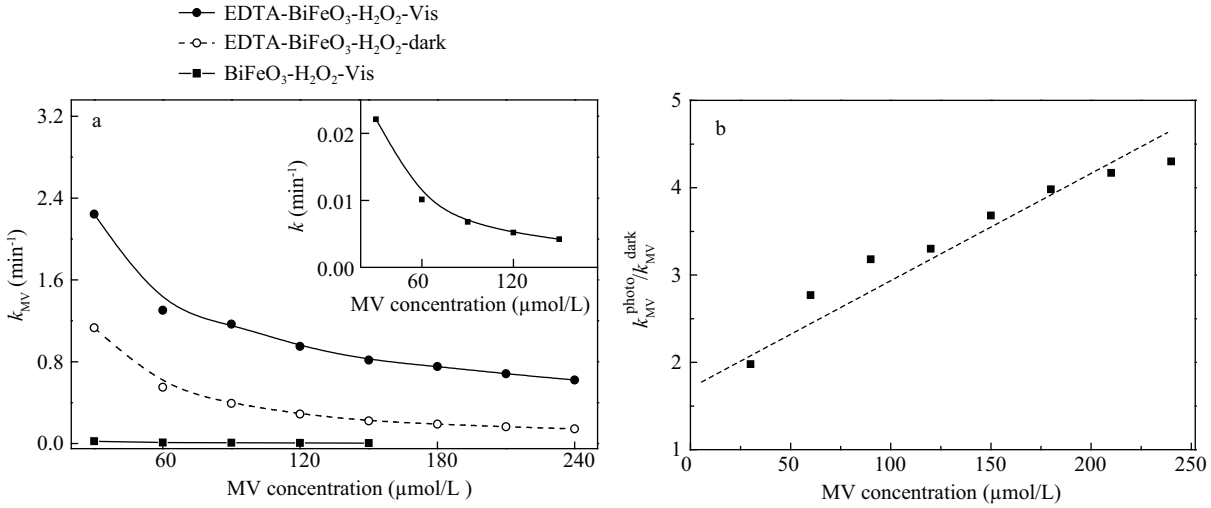

Fig. 6 (a) Effects of initial MV concentration on the pseudo first-order rate constant (k_{MV}) of the MV degradation in different systems, (b) effects of initial MV concentration on the ratio of k_{MV} in the EDTA-$BiFeO_3$-H_2O_2-Vis system (k_{MV}^{photo}) to that in the EDTA-$BiFeO_3$-H_2O_2-dark system (k_{MV}^{dark}). Reaction conditions: $BiFeO_3$ load 0.5 g/L, H_2O_2 concentration 20 mmol/L, EDTA concentration 0.4 mmol/L, pH 5, and temperature 25°C.

in systems of ligand-$BiFeO_3$-H_2O_2 both with and without visible light irradiation (**Fig. 7**). This is due to the following two reasons: firstly, the added EDTA and NTA favor the activation of H_2O_2 and the generation of OH radicals; secondly, the ligand as an organic compound reacts competitively with OH radicals, leading to a partial inhibition of the MV degradation. Moreover, at each tested concentration of ligand, the degradation of MV in the NTA-$BiFeO_3H_2O_2$-Vis system was much faster than that in the dark under similar experimental conditions. These observations strongly support the hypothesis that the *in situ* surface modification of $BiFeO_3$ nanoparticles by EDTA or NTA could greatly enhance the photocatalytic degradation of organic pollutants at high concentrations in the presence of H_2O_2. Research work is currently going on in our laboratory in order to further clarify the molecular mechanism of the enhancement effect of ligands on the photocatalytic performance of $BiFeO_3$ nanoparticles.

We also compared the visible light photocatalytic ability of nano-$BiFeO_3$ and nano-Bi_2WO_6 (**Fig. S3**), because Bi_2WO_6 nanoplates were reported to be an excellent photocatalytic material under visible light irradiation (Zhang and Zhu, 2005). After Bi_2WO_6 nanoplates were prepared through a hydrothermal process, the degradation of MV was studied in the systems EDTA-$BiFeO_3$-H_2O_2-Vis and EDTA-Bi_2WO_6-H_2O_2-Vis. It was found that the degradation of MV in the $BiFeO_3$ system was much faster than that in the Bi_2WO_6 system: the former produced a MV removal of 90% in 0.5 min, whereas the latter yielded a MV removal of only 50% in 90 min. This further confirms that nano-$BiFeO_3$ is an excellent visible light Fentonlike responsive photocatalyst.

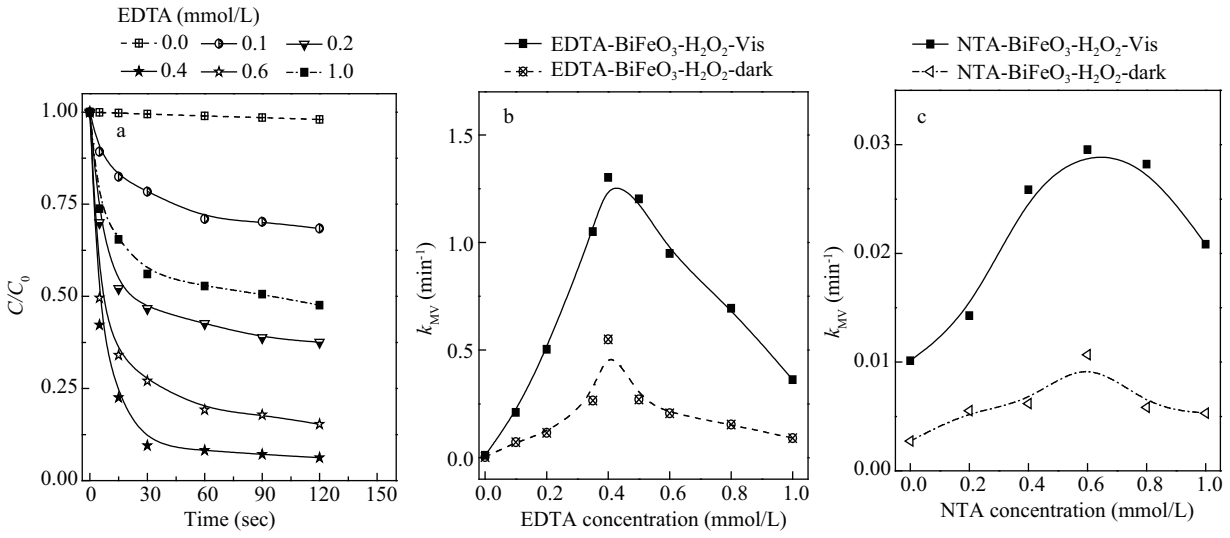

Fig. 7 (a) Degradation of MV in the $BiFeO_3$-H_2O_2-Vis system with EDTA addition, (b, c) effects of initial concentrations of EDTA (b) and NTA (c) on k_{MV} in the ligand-$BiFeO_3$-H_2O_2 system in the dark and under visible light irradiation. Reaction conditions: $BiFeO_3$ load 0.5 g/L, MV concentration 60 μmol/L, H_2O_2 concentration 20 mmol/L, pH 5.0, and temperature 25°C.

2.5 Stability and reusability of $BiFeO_3$ under visible light irradiation

In experiments on degradation under visible light irradiation, it is very important to evaluate whether $BiFeO_3$ is stable in the presence of EDTA, because the complexation effects of small molecule carboxylic acids may induce the dissolution of Fe^{3+} from iron oxide surfaces (Casey and Ludwig, 1996; Loring et al., 2008) and both NTA and EDTA are small molecule carboxylic acids. We monitored the amount of leached Fe^{3+} and Bi^{3+} with AAS during the degradation experiment at pH 5.0 (**Fig. S4a**) and found that no Bi^{3+} was detected and the detected Fe^{3+} concentration was also very low (only 1.50% and 1.59% of Fe was leached to the solution in the presence of EDTA and NTA, respectively) under visible light irradiation. This means that $BiFeO_3$ was stable during the degradation experiments.

The recyclability of $BiFeO_3$ was evaluated by successive batch experiments of MV degradation in the $BiFeO_3$-EDTA-H_2O_2-Vis system. In the degradation experiments, the recycled $BiFeO_3$ was used with simultaneous addition of EDTA. It was found that the composite was able to be reutilized for at least five cycles, and the rate constant for the MV degradation was estimated to be 1.30, 1.28, 1.28, 1.27 and 1.27 min^{-1} for the initial five cycles (**Fig. S4b**). Because the reused catalyst retained catalytic activity almost as efficient as fresh material, it may be concluded that $BiFeO_3$ could be recycled effectively.

2.6 Consumption of H_2O_2 and EDTA in the reaction system

We monitored the concentration of H_2O_2 during the degradation of pollutants in the systems of $BiFeO_3$-NTA-H_2O_2-Vis and $BiFeO_3$-H_2O_2-EDTA-Vis (**Fig. S5a**). It was found that about 30% and 55% H_2O_2 was decomposed in the systems of $BiFeO_3$-H_2O_2-Vis and $BiFeO_3$NTA-H_2O_2-Vis, respectively, after 120 min. About 98% of H_2O_2 was consumed in the $BiFeO_3$-H_2O_2-EDTA-Vis system after 20 min, which was much faster than the former two systems. The sequence of the decomposition rate of H_2O_2 was in the order $BiFeO_3$-H_2O_2-Vis < $BiFeO_3$-NTA-H_2O_2-Vis < $BiFeO_3$-H_2O_2-EDTA-Vis, accounting for the observation that the degradation efficiency of pollutants in the $BiFeO_3$-H_2O_2-EDTA-Vis system was much higher than in the other reaction systems. The fast decomposition rate of H_2O_2 also greatly reduces its potential unfriendly impact on the environment. The relationship of MV degradation and H_2O_2 consumption was explored (**Fig. S5b**): H_2O_2 was decomposed rapidly during the degradation of MV, and the fast decomposition of H_2O_2 produced more hydroxyl radicals, promoting the degradation of MV.

The above experimental results confirmed that the introduction of NTA and EDTA resulted in remarkable enhancement of the degradation efficiency of the pollutants, with EDTA exhibiting a much stronger effect than NTA. Therefore, we used EDTA to modify the surface of $BiFeO_3$ and monitored the concentration of EDTA during the degradation experiment (**Fig. S5c**). It was found that the concentration of EDTA was decreased as reaction time progressed. In the absence of MV, about 90% of EDTA was removed in 30 min, suggesting that EDTA could be degraded by hydroxyl radicals. In the presence of MV, 80% of EDTA was degraded in 30 min. It was clearly shown that both MV and EDTA could be degraded in the $BiFeO_3$EDTA-H_2O_2-Vis system. This means that any adverse impact of EDTA on the environment in the reaction system would be slight. Besides, it is a promising development that EDTA could be disposed in coordination with other pollutants.

2.7 A mechanism for ·OH radical generation in EDTA-$BiFeO_3$-H_2O_2-Vis system

A mechanism for ·OH radical generation in the EDTA-$BiFeO_3$-H_2O_2Vis system was proposed. The degradation of pollutions in the system is caused by ·OH radicals, which are generated by both the photocatalytic process and Fenton-like process. The hydroxyl radicals are produced through two pathways in the photocatalytic process. In the first pathway, ·OH radicals are generated from the reaction between photo-induced electrons and H_2O_2 (Reaction (1)); in the second one, they come from the reaction of free radicals with dissolved O_2. As the EDTA-$BiFeO_3$-H_2O_2 system is exposed to visible light irradiation, the $BiFeO_3$-EDTA surface complexes ($\equiv Fe^{III}(RCO_2)^{2+}$) may be excited to form free radicals (R·) through intramolecular ligand-to-metal charge transfer (Reaction (4)). The R· radicals react with dissolved O_2 to generate intermediates that form additional Fe^{3+} complexes and contribute to the $\equiv Fe^{III}/\equiv Fe^{II}$ cycle and the production of ·OH (Reactions (5) and (6)) (Ghiselli et al., 2004). Therefore, the oxidizing ability of the EDTA-$BiFeO_3$-H_2O_2 system is further enhanced by the introduction of visible light irradiation. It should be pointed out that even in the absence of H_2O_2, Reactions (5) and (6) can occur in the visible light-irradiated EDTA-$BiFeO_3$ system. Thus, the addition of EDTA or NTA alone also improved considerably the degradation of MV in $BiFeO_3$ dispersions without H_2O_2 under visible light irradiation.

$$\equiv Fe^{III}(RCO_2)^{2+} + h\nu \longrightarrow \equiv Fe^{II} + CO_2 + R\cdot \quad (4)$$

$$R\cdot + O_2 \longrightarrow ROO\cdot \longrightarrow \text{oxidzed products} \quad (5)$$

$$\text{Oxidized products} + \equiv Fe^{III} \longrightarrow \cdot OH + \equiv Fe^{II} \quad (6)$$

$$\equiv Fe^{II} + H_2O_2 \longrightarrow \equiv Fe^{III} + \cdot OH + OH^- \quad (7)$$

In addition to the photocatalytic process, the hydroxyl radicals are also generated from a Fenton-like reaction in

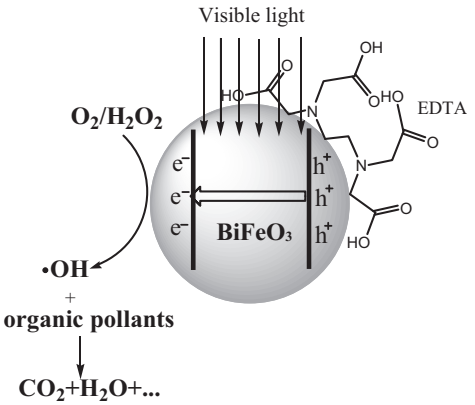

Fig. 8 A proposed mechanism for the visible light Fentonlike process of $BiFeO_3$.

the system EDTA-$BiFeO_3$-H_2O_2-Vis. The process may be described as follows: first, EDTA molecules are absorbed on the surface of $BiFeO_3$, forming a complex (≡Fe^{III}-EDTA) as shown in Reaction (8). Next, the ≡Fe^{III}-EDTA complex reacts with H_2O_2, generating a ferrous complex (Fe^{II}-EDTA) and $\cdot HO_2$ (Reactions (9) and (10)). Then the Fe^{II}-EDTA complex reacts with H_2O_2 and generates hydroxyl radicals. Therefore, the Fenton-like reaction could also be improved remarkably by adding EDTA. In fact, Kwon et al. (2009) investigated the decomposition of pentachlorophenol by an electron beam process enhanced in the presence of Fe(III)-EDTA, and reported that the introduction of EDTA caused the $\cdot HO_2/\cdot O_2$ -driven Fenton-like reaction to produce much more ·OH, which is significant for the complete degradation of pentachlorophenol. Finally, the ·OH radicals generated from both the photocatalytic process and Fenton-like process degrade organic pollutants to harmless products (Eq. (12)). The above mechanism is illustrated by **Fig. 8**.

$$\equiv Fe^{III} + EDTA \longrightarrow \equiv Fe^{III}\text{-}EDTA \quad (8)$$

$$\equiv Fe^{III}\text{-}EDTA + H_2O_2 \longrightarrow \equiv Fe^{II}\text{-}EDTA + H^+ + \cdot HO_2 \quad (9)$$

$$\equiv Fe^{III}\text{-}EDTA + \cdot HO_2 \longrightarrow \equiv Fe^{II}\text{-}EDTA + O_2 + H^+ \quad (10)$$

$$\equiv Fe^{II}\text{-}EDTA + H_2O_2 \longrightarrow \equiv Fe^{III}\text{-}EDTA + \cdot OH + OH^- \quad (11)$$

$$\text{Organic pollutants} + \cdot OH \longrightarrow \cdots \longrightarrow CO_2 + H_2O \quad (12)$$

3 Conclusions

$BiFeO_3$ nanoparticles are able to catalytically activate H_2O_2 for the decomposition of organic pollutants in the dark, but their catalytic ability is rather weak towards more resistant organic pollutants. Visible light irradiation was utilized to improve the catalytic ability of $BiFeO_3$ nanoparticles in the present work. Under optimized conditions, the apparent degradation rate constant of MV (30 μmol/L) in the $BiFeO_3$-H_2O_2 system was increased from 6.37×10^{-3} min^{-1} in the dark to 2.21×10^{-2} min^{-1} under visible light irradiation. Furthermore, we proposed a new approach to increase the visible light photo-Fentonlike catalytic ability of $BiFeO_3$ nanoparticles by *in situ* surface modification. It was observed that a small addition of EDTA (0.4 mmol/L) into the $BiFeO_3$-H_2O_2-Vis system increased the apparent degradation rate constant of MV (60 μmol/L) by 128 fold, from 1.01×10^2 to 130 min^{-1}. It was also found that EDTA could be decomposed rapidly during the degradation of MV, which eliminated its possible unfriendly impact on the environment. This may suggest an additional benefit, that EDTA could be disposed in coordination with other pollutants in our reaction system. In addition, it was confirmed that MV at high concentrations was degraded more effectively in the EDTA-$BiFeO_3$-H_2O_2-Vis system than in the EDTA-$BiFeO_3$-H_2O_2-dark system. The strong enhancement effect may enable additional promising applications of $BiFeO_3$ nanoparticles as a visible light photo-Fentonlike catalyst for the removal of organic pollutants from wastewaters.

Acknowledgments

This work was supported by the National Science Foundation of China (No. 21077037, 21177044, 81030051). The Analytical and Testing Center of Huazhong University of Science and Technology is thanked for their assistance in the characterization of the catalysts.

Supporting materials

Supplementary data associated with this article can be found in the online version.

References

Bader H, Sturzenegger V, Hoigné J, 1988. Photometric method for the determination of low concentrations of hydrogen peroxide by the peroxidase catalyzed oxidation of N, N-diethyl-*p*-phenylenediamine (DPD). *Water Research*, 22(9): 1109–1115.

Bremner D H, Molina R, Martínez F, Melero J A, Segura Y, 2009. Degradation of phenolic aqueous solutions by high frequency sono-Fenton systems (US-Fe_2O_3/SBA15-H_2O_2). *Applied Catalysis B-Environmental*, 90(3-4): 380–388.

Cai T J, Liao Y C, Peng Z S, Long Y F, Wei Z Y, Deng Q, 2009. Photocatalytic performance of TiO_2 catalysts modified by $H_3PW_{12}O_{40}$, ZrO_2 and CeO_2. *Journal of Environmental Sciences*, 21(7): 997–1004.

Canle-L M, Santaballa J A, Vulliet E, 2005. On the mechanism of TiO_2-photocatalyzed degradation of aniline derivatives. *Journal of Photochemistry and Photobiology A: Chemistry*, 175(2-3): 192–200.

Casey W H, Ludwig C, 1996. The mechanism of dissolution of

oxide minerals. *Nature*, 381(6582): 506–509.

Catrinescu C, Teodosiu C, Macoveanu M, Miehe-Brendlé J, Dred R L, 2003. Catalytic wet peroxide oxidation of phenol over Fe-exchanged pillared beidellite. *Water Research*, 37(5): 1154–1160.

Chen F, Xie Y D, He J J, Zhao J C, 2001. Photo-Fenton degradation of dye in methanolic solution under both UV and visible irradiation. *Journal of Photochemistry and Photobiology A: Chemistry*, 138(2): 139–146.

Cheng M M, Ma W H, Li J, Huang Y P, Zhao J C Wen Y X et al., 2004. Visiblelight-assisted degradation of dye pollutants over Fe(III)-loaded resin in the presence of H_2O_2 at neutral pH values. *Environmental Science and Technology*, 38(5): 1569–1575.

Deng J H, Jiang J Y, Zhang Y Y, Lin X P, Du C M, Xiong Y, 2008. $FeVO_4$ as a highly active heterogeneous Fenton-like catalyst towards the degradation of orange II. *Applied Catalysis B-Environmental*, 84(3-4): 468–473.

Dwyer J, Kavanagh L, Lant P, 2008. The degradation of dissolved organic nitrogen associated with melanoidin using a UV/H_2O_2 AOP. *Chemosphere*, 71(9): 1745–1753.

Feng J Y, Hu X J, Yue P L, 2004. Degradation of salicylic acid by photo-assisted Fenton reaction using Fe ions on strongly acidic ion exchange resin as catalyst. *Chemical Engineering Journal*, 100(1-3): 159–165.

Fu H B, Pan C S, Yao W Q, Zhu Y F, 2005. Visible-light-induced degradation of rhodamine B by nanosized Bi_2WO_6. *Journal of Physical Chemistry B*, 109(47): 22432–22439.

Gao F, Chen X Y, Yin K B, Dong S, Ren Z F, Yuan F et al., 2007. Visible-light photocatalytic properties of weak magnetic $BiFeO_3$ nanoparticles. *Advanced Materials*, 19(19): 2889–2892.

Gao X D, Metge D W, Ray C, 2009. Surface complexation of carboxylate adheres *Cryptosporidium parvum* öocysts to the hematite-water interface. *Environmental Science and Technology*, 43(19): 7423–7429.

Ghiselli G, Jardim W F, Litter M I, Mansilla H D, 2004. Destruction of EDTA using Fenton and photo-Fenton-like reactions under UV-A irradiation. *Journal of Photochemistry and Photobiology A: Chemistry*, 167(1): 59–67.

Guan H M, Zhu L H, Zhou H H, Tang H Q, 2008. Rapid probing of photocatalytic activity on titania-based self-cleaning materials using 7-hydroxycoumarin fluorescent probe. *Analytica Chimica Acta*, 608(1): 73–78.

Guan X H, Chen G H, Shang C, 2007. ATR-FT-IR and XPS study on the structure of complexes formed upon the adsorption of simple organic acids on aluminum hydroxide. *Journal of Environmental Sciences*, 19(4): 438–443.

Guimaraes I R, Giroto A, Oliveira L C A, Guerreiro M C, Lima D Q, Fabris J D, 2009. Synthesis and thermal treatment of Cu-doped goethite: oxidation of quinoline through heterogeneous Fenton process. *Applied Catalysis B- Environmental*, 91(3-4): 581–586.

Guo L Q, Chen F, Fan X Q, Cai W D, Zhang J L, 2010a. S-doped-Fe_2O_3 as a highly active heterogeneous Fenton-like catalyst towards the degradation of acid orange 7 and phenol. *Applied Catalysis B-Environmental*, 96(1-2): 162–168.

Guo R Q, Fang L, Dong W, Zheng F A, Shen M R, 2010b. Enhanced photocatalytic activity and ferromagnetism in Gd doped $BiFeO_3$ nanoparticles. *Journal of Physical Chemistry C*, 114(49): 21390–21396.

Han Y F, Phonthammachai N, Ramesh K, Zhong Z Y, White T, 2008. Removing organic compounds from aqueous medium via wet peroxidation by gold catalysts. *Environmental Science and Technology*, 42(3): 908–912.

He Z, Yang S G, Ju Y M, Sun C, 2009. Microwave photocatalytic degradation of Rhodamine B using TiO_2 supported on activated carbon: Mechanism implication. *Journal of Environmental Sciences*, 21(2): 268–272.

Heckert E G, Seal S, Self W T, 2008. Fenton-like reaction catalyzed by the rare earth inner transition metal cerium. *Environmental Science and Technology*, 42(13): 5014–5019.

Huo Y N, Jin Y, Zhang Y, 2010. Citric acid assisted solvothermal synthesis of $BiFeO_3$ microspheres with high visible-light photocatalytic activity. *Journal of Molecular Catalysis A-Chemical*, 331(1-2): 15–20.

Kwon B G, Kim E J, Lee J H, 2009. Pentachlorophenol decomposition by electron beam process enhanced in the presence of Fe(III)-EDTA. *Chemosphere*, 74(10): 1335–1339.

Li S, Lin Y H, Zhang B P, Nan C W, Wang Y, 2009. Photocatalytic and magnetic behaviors observed in nanostructured $BiFeO_3$ particles. *Journal of Applied Physics*, 105(5): 056105.

Li Y C, Bachas L G, Bhattacharyya D, 2005. Kinetics studies of trichlorophenol destruction by chelate-based Fenton reaction. *Environmental Engineering Science*, 22(6): 756–771.

Liu Z K, Qi Y J, Lu C J, 2010. High efficient ultraviolet photocatalytic activity of $BiFeO_3$ nanoparticles synthesized by a chemical coprecipitation process. *Journal of Materials Science-Materials in Electronics*, 21(4): 380–384.

Loring J S, Simanova A A, Persson P, 2008. Highly mobile iron pool from a dissolution-readsorption process. *Langmuir*, 24(14): 7054–7057.

Luo W, Li Y S, Yuan J, Zhu L H, Liu Z D, Tang H Q et al., 2010a. Ultrasensitive fluorometric determination of hydrogen peroxide and glucose by using multiferroic $BiFeO_3$ nanoparticles as a catalyst. *Talanta*, 81(3): 901–907.

Luo W, Zhu L H, Wang N, Tang H Q, Cao M J, She Y B, 2010b. Efficient removal of organic pollutants with magnetic nanoscaled $BiFeO_3$ as a reusable heterogeneous Fenton-like catalyst. *Environmental Science and Technology*, 44(5): 1786–1791.

Ma Y S, Sung C F, Lin J G, 2010. Degradation of carbofuran in aqueous solution by ultrasound and Fenton processes: effect of system parameters and kinetic study. *Journal of Hazardous Materials*, 178(1-3): 320–325.

Malato S, Blanco J, Alarcón D C, Maldonado M I, Fernández-Ibáñez P, Gernjak W, 2007. Photocatalytic decontamination and disinfection of water with solar collectors. *Catalysis Today*, 122(1-2): 137–149.

Monteagudo J M, Durán A, López-Almodóvar C, 2008. Homogenous ferrioxalateassisted solar photo-Fenton degradation of orange II aqueous solutions. *Applied Catalysis B-Environmental*, 83(1-2): 46–55.

Nam S, Renganthan V, Tratnyek P G, 2001. Substituent effects on azo dye oxidation by the Fe^{III}-EDTA-H_2O_2 system. *Chemosphere*, 45(1): 59–65.

Neamtu M, Zaharia C, Catrinescu C, Yediler A, Macoveanu M, Kettrup A, 2004. Fe-exchanged Y zeolite as catalyst for wet

peroxide oxidation of reactive azo dye Procion Marine H-EXL. *Applied Catalysis B: Environmental*, 48(4): 287–294.

Rastogi A, Al-Abed S R, Dionysiou D D, 2009. Effect of inorganic, synthetic and naturally occurring chelating agents on Fe(II) mediated advanced oxidation of chlorophenols. *Water Research*, 43(3): 684–694.

Roy G, de Donato P, Görner T, Barres O, 2003. Study of tropaeolin degradation by iron-proposition of a reaction mechanism. *Water Research*, 37(20): 4954–4964.

Seitelska G V, Gallios G P, Zouboulis A I, 2004. Sonochemical decomposition of natural polyphenolic compound (condensed tannin). *Chemosphere*, 56(10): 981–987.

Tokumura M, Znad H T, Kawase Y, 2008. Decolorization of dark brown colored coffee effluent by solar photo-Fenton reaction: effect of solar light dose on decolorization kinetics. *Water Research*, 42(18): 4665–4673.

Tryba B, Piszcz M, Grzmil B, Pattek-Janczykb A, Morawski A W, 2009. Photodecomposition of dyes on Fe-C-TiO_2 photocatalysts under UV radiation supported by photo-Fenton process. *Journal of Hazardous Materials*, 162(1): 111–119.

Ventura A, Jacquet G, Bermond A, Camel V, 2002. Electrochemical generation of the Fenton's reagent: application to atrazine degradation. *Water Research*, 36(14): 3517–3522.

Wang N, Zhu L H, Deng K J, She Y B, Yu Y M, Tang H Q, 2010. Visible light photocatalytic reduction of Cr(VI) on TiO_2 *in situ* modified with small molecular weight organic acids. *Applied Catalysis B: Environmental*, 95(3-4): 400–407

Wang N, Zhu L H, Huang Y P, She Y B, Yu Y M, Tang H Q, 2009. Drastically enhanced visible-light photocatalytic degradation of colorless aromatic pollutants over TiO_2 via a charge-transfer-complex path: A correlation between chemical structure and degradation rate of the pollutants. *Journal of Catalysis*, 266(2): 199–206.

Xue X F, Hanna K, Despas C, Wu F, Deng N S, 2009. Effect of chelating agent on the oxidation rate of PCP in the magnetite/H_2O_2 system at neutral pH. *Journal of Molecular Catalysis A: Chemical*, 311(1-2): 29–35.

Yang Y, Wang P, Shi S J, Liu Y, 2009. Microwave enhanced Fenton-like process for the treatment of high concentration pharmaceutical wastewater. *Journal of Hazardous Materials*, 168(1): 238–245.

Yu J G, Yu H G, Cheng B, Zhao X J, Yu J C, Ho W K, 2003. The effect of calcination temperature on the surface microstructure and photocatalytic activity of TiO_2 thin films prepared by liquid phase deposition. *Journal of Physical Chemistry B*, 107(50): 13871–13879.

Yuan S H, Tian M, Cui Y P, Lin L, Lu X H, 2006. Treatment of nitrophenols by cathode reduction and electro-Fenton methods. *Journal of Hazardous Materials*, 137(1): 573–580.

Zepp R G, Faust B C, Holgne J, 1992. Hydroxyl radical formation in aqueous reactions (pH 38) of iron(II) with hydrogen peroxide: the photo-Fenton reaction. *Environmental Science and Technology*, 26(2): 313–319.

Zhang C, Zhu Y F, 2005. Synthesis of square Bi_2WO_6 nanoplates as high-activity visible-light-driven photocatalysts. *Chemistry of Materials*, 17(13): 3537–3545.

Zhang J B, Zhuang J, Gao L Z, Zhang Y, Gu N, Feng J et al., 2008. Decomposing phenol by the hidden talent of ferromagnetic nanoparticles. *Chemosphere*, 73(9): 1524–1528.

Zhang J W, Fu D F, Xu Y D, Liu C Y, 2010. Optimization of parameters on photocatalytic degradation of chloramphenicol using TiO_2 as photocatalyist by response surface methodology. *Journal of Environmental Sciences*, 22(8): 1281–1289.

Supporting materials

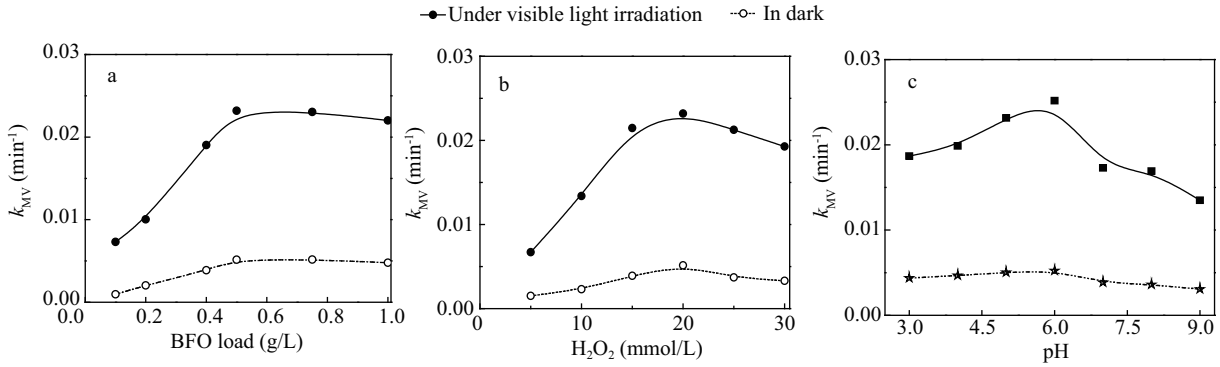

Fig. S1 Effects of catalyst load (a), initial H_2O_2 concentration (b) and solution pH (c) on the apparent degradation constant of MV (30 μmol/L) in the presence of $BiFeO_3$ nanoparticles (0.5 g/L) under visible light irradiation and in dark. Reaction conditions: initial H_2O_2 concentration 20 mmol/L, pH 5.0, and temperature 25°C.

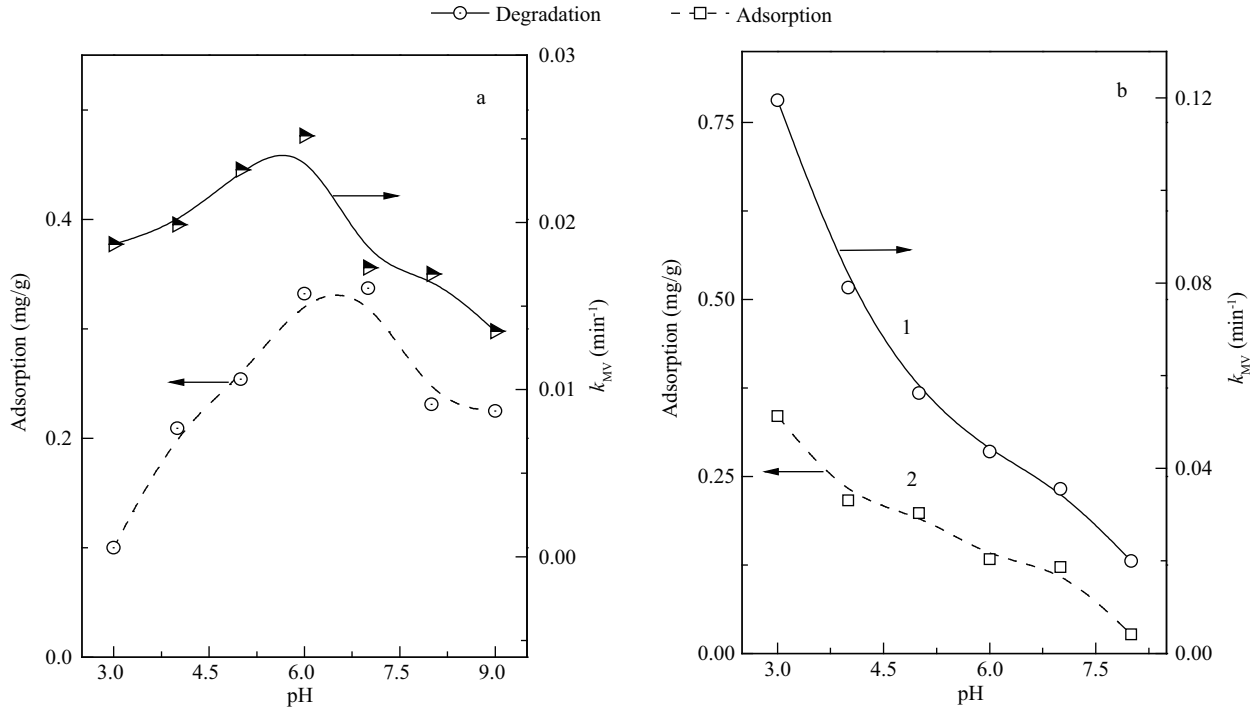

Fig. S2 Photo-Fenton like catalytic degradation rate constant and dark adsorption of (a) MV (30 μmol/L) and (b) RhB (10 μmol/L) in the presence of $BiFeO_3$ (0.5 g/L) and H_2O_2 (20 mmol/L).

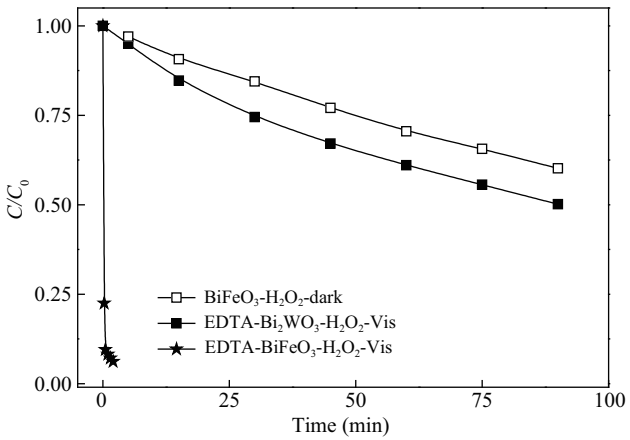

Fig. S3 Degradation of MV (60 μmol/L) in the systems of Bi_2WO_6-H_2O_2-Vis, EDTA-Bi_2WO_6-H_2O_2-Vis and EDTA-$BiFeO_3$-H_2O_2-Vis. Reaction conditions: $BiFeO_3$ (or Bi_2WO_6) load 0.5 g/L, H_2O_2 concentration 20 mmol /L, EDTA concentration 0.4 mmol/L, pH 5, and temperature 25°C.

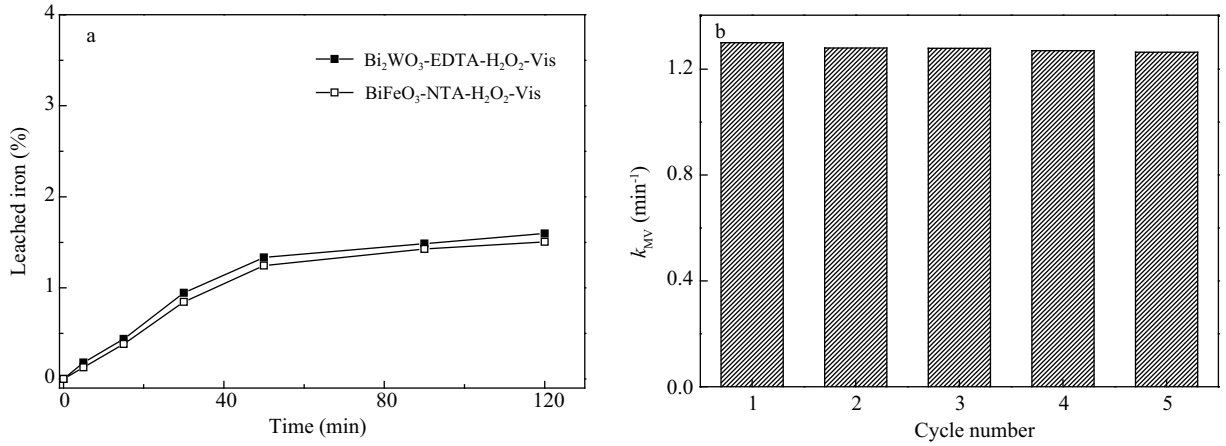

Fig. S4 (a) Percentage of total dissolved iron during the degradation in the $BiFeO_3$-NTA-H_2O_2-Vis and $BiFeO_3$-EDTA-H_2O_2-Vis systems. (b) Degradation of MV with the recycled $BiFeO_3$. Reaction conditions: $BiFeO_3$ load 0.5 g/L, NTA concentration: 0.6 mmol/L, EDTA concentration: 0.4 mmol/L, MV concentration 60 μmmol/L, H_2O_2 concentration 20 mmol/L, pH 5.0, and temperature 25°C.

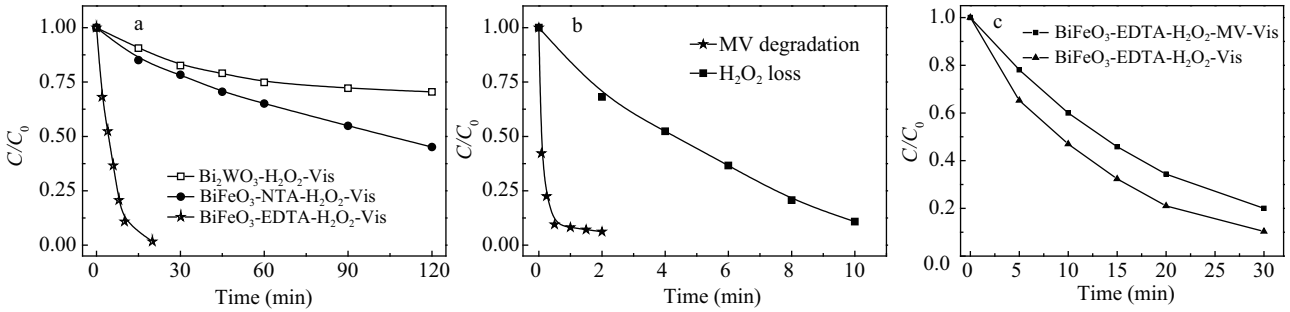

Fig. S5 (a) H_2O_2 loss in the systems of $BiFeO_3$-H_2O_2-Vis, $BiFeO_3$-NTA-H_2O_2-Vis and $BiFeO_3$-H_2O_2-EDTA -Vis. (b) H_2O_2 loss and the degradation of MV in the $BiFeO_3$-H_2O_2-EDTA-Vis system. (c) EDTA loss in the systems of $BiFeO_3$-EDTA-H_2O_2-MV-Vis and $BiFeO_3$-EDTA-H_2O_2-Vis. Reaction conditions: $BiFeO_3$ load 0.5 g/L, NTA concentration: 0.6 mmol/L, EDTA concentration: 0.4 mmol/L, MV concentration 60 μmol/L, H_2O_2 concentration 20 mmol/L, pH 5.0, and temperature 25°C.

JOURNAL OF ENVIRONMENTAL SCIENCES

环境科学学报(英文版)

(http://www.jesc.ac.cn)

Aims and scope

Journal of Environmental Sciences is an international academic journal supervised by Research Center for Eco-Environmental Sciences, Chinese Academy of Sciences. The journal publishes original, peer-reviewed innovative research and valuable findings in environmental sciences. The types of articles published are research article, critical review, rapid communications, and special issues.

The scope of the journal embraces the treatment processes for natural groundwater, municipal, agricultural and industrial water and wastewaters; physical and chemical methods for limitation of pollutants emission into the atmospheric environment; chemical and biological and phytoremediation of contaminated soil; fate and transport of pollutants in environments; toxicological effects of terrorist chemical release on the natural environment and human health; development of environmental catalysts and materials.

For subscription to electronic edition

Elsevier is responsible for subscription of the journal. Please subscribe to the journal via http://www.elsevier.com/locate/jes.

For subscription to print edition

China: Please contact the customer service, Science Press, 16 Donghuangchenggen North Street, Beijing 100717, China. Tel: +86-10-64017032; E-mail: journal@mail.sciencep.com, or the local post office throughout China (domestic postcode: 2-580).

Outside China: Please order the journal from the Elsevier Customer Service Department at the Regional Sales Office nearest you.

Submission declaration

Submission of an article implies that the work described has not been published previously (except in the form of an abstract or as part of a published lecture or academic thesis), that it is not under consideration for publication elsewhere. The submission should be approved by all authors and tacitly or explicitly by the responsible authorities where the work was carried out. If the manuscript accepted, it will not be published elsewhere in the same form, in English or in any other language, including electronically without the written consent of the copyright-holder.

Submission declaration

Submission of the work described has not been published previously (except in the form of an abstract or as part of a published lecture or academic thesis), that it is not under consideration for publication elsewhere. The publication should be approved by all authors and tacitly or explicitly by the responsible authorities where the work was carried out. If the manuscript accepted, it will not be published elsewhere in the same form, in English or in any other language, including electronically without the written consent of the copyright-holder.

Editorial

Authors should submit manuscript online at http://www.jesc.ac.cn. In case of queries, please contact editorial office, Tel: +86-10-62920553, E-mail: jesc@263.net, jesc@rcees.ac.cn. Instruction to authors is available at http://www.jesc.ac.cn.

Journal of Environmental Sciences (Established in 1989)

Vol. 25 No. 6 2013

Supervised by	Chinese Academy of Sciences	**Published by**	Science Press, Beijing, China
Sponsored by	Research Center for Eco-Environmental		Elsevier Limited, The Netherlands
	Sciences, Chinese Academy of Sciences	**Distributed by**	
Edited by	Editorial Office of Journal of	Domestic	Science Press, 16 Donghuangchenggen
	Environmental Sciences		North Street, Beijing 100717, China
	P. O. Box 2871, Beijing 100085, China		Local Post Offices through China
	Tel: 86-10-62920553; http://www.jesc.ac.cn	Foreign	Elsevier Limited
	E-mail: jesc@263.net, jesc@rcees.ac.cn		http://www.elsevier.com/locate/jes
Editor-in-chief	Hongxiao Tang	**Printed by**	Beijing Beilin Printing House, 100083, China

CN 11-2629/X **Domestic postcode: 2-580** **Domestic price per issue RMB ¥ 110.00**

ISSN 1001-0742